CrossMark

Eddy diffusivity: a single dispersion analysis of high resolution drifters in a tidal shallow estuary

Kabir Suara[1] · Richard Brown[1] · Michael Borgas[2]

Abstract In an estuary, mixing and dispersion resulting from turbulence and small scale fluctuation has strong spatio-temporal variability which cannot be resolved in conventional hydrodynamic models while some models employs parameterizations large water bodies. This paper presents small scale diffusivity estimates from high resolution drifters sampled at 10 Hz for periods of about 4 h to resolve turbulence and shear diffusivity within a tidal shallow estuary (depth <3 m). Taylor's diffusion theorem forms the basis of a first order estimate for the diffusivity scale. Diffusivity varied between 0.001 and 0.02 m^2/s during the flood tide experiment. The diffusivity showed strong dependence ($R^2 > 0.9$) on the horizontal mean velocity within the channel. Enhanced diffusivity caused by shear dispersion resulting from the interaction of large scale flow with the boundary geometries was observed. Turbulence within the shallow channel showed some similarities with the boundary layer flow which include consistency with slope of 5/3 predicted by Kolmogorov's similarity hypothesis within the inertial subrange. The diffusivities scale locally by 4/3 power law following Okubo's scaling and the length scale scales as 3/2 power law of the time scale. The diffusivity scaling herein suggests that the modelling of small scale mixing within tidal shallow estuaries can be approached from classical turbulence scaling upon identifying pertinent parameters.

✉ Kabir Suara
k.suara@qut.edu.au

[1] Science and Engineering Faculty, Queensland University of Technology, 2 George St., Brisbane, QLD 4000, Australia

[2] Marine and Atmospheric Research, Commonwealth Scientific and Industrial Research Organisation (CSIRO), Aspendale, VIC 3195, Australia

1 Introduction

In estuaries and natural water channels, the estimate of velocity and diffusion coefficients is important to the modelling of scalar transport and mixing. Estuarine management requires understanding of circulation to predict the transport of scalars for water quality monitoring (e.g. salinity distribution and chlorophyll level), pollution run-off tracking (e.g. waste water and accidental spillage) and ecosystem monitoring (e.g. larvae and algae transport). These management strategies rely on a combination of historical observations of tide and wind quantities, river and ocean conditions, bathymetry and results from numerical modelling. Numerical models require velocity fluctuations and dispersion coefficients for parameterising processes occurring at unresolved scales. Therefore these quantities are fundamental to estuarine managements. Direct measurement of these quantities is rarely available at time scales less than a tidal cycle in shallow water estuaries where reasonably high frequency measurements are required to resolve turbulence and shear dispersion. Parameterization of diffusivity (30 m–100 km) obtained from large water bodies [1, 2] might not be applicable because of difference in scale of processes (O[1 m]) causing mixing and unsteadiness of shallow estuaries particularly at time scales less than a tidal period.

Transport in estuaries is a complex phenomenon due to the transition and strong competition between ocean and river. The transport of scalars is characterized by tidal currents, energetic turbulence, and rough bathymetry among other factors [3]. In an estuary, mixing is caused by the combination of tidal scale advection in mean flow and small scale processes that could be termed turbulence diffusion. Fischer et al. [4] identified the mechanisms causing chaos in estuaries to be related to a combination of one or more of three of the wind, the tide and the river. This combination results in long term fluctuations in scalar and vector properties. These mechanisms induce variation in important properties such as density, temperature, salinity, PH, dissolved oxygen velocity etc. in all directions leading to various degrees of mixing (well or partially mixed), stratification and destratification. MacCready and Geyer [3] suggested that the key dynamic role of length of salt intrusion was apparent in many past observations. All these effects have led to varying degree of estimate of diffusivities across different locations particularly at scales in order of a tidal period. For example Riddle and Lewis [5] reported the lateral mixing from dye tracer experiments in the UK water with minimum values which ranged from 0.003 and 0.42 m^2/s. Their results revealed a distinct band showing shallower water with an order of magnitude reduction in vertical mixing possibly restricted by the size of eddies [5].

A recent investigative tool for estuaries based on Lagrangian method is the use of GPS-tracked Lagrangian drifters. Drifters have been applied to study the underlying fluid dynamics and scalar particle dispersion at various scales in oceans [6], seas [7, 8], lakes [9], large estuaries [10] and recently tidal inlet [11]. While these previous studies focussed on the relatively large scale processes defined by their domain size and spatio-temporal resolution of available instruments, small scale processes [O (100 s) and O (few metres)] have rarely been studied. Recent improvements in GPS technology have paved the way for the development of high resolution Lagrangian drifters to study dispersion in shallow waters [with depth ∼O (few metres)], where processes of interest occur in small scales [O (100 s) and O (few metres)] [12]. In order to quantify small scale eddy diffusivity and it variability with particular focus on period less than a tidal cycle, high resolution GPS-tracked drifters were released from the inlet of Eprapah Creek, a shallow tidal estuary, eastern Australia.

The use of high resolution tracked particles to study dispersion in shallow waters have many advantages when compared with existing dye tracer technology and acoustic Eulerian devices, including flexibility of usage, lower cost, and higher spatial coverage [12]. Despite these advantages, there are some clear limitations. One methodological limitation is that surface drifter application to shallow tidal estuaries only captures quasi-2D processes, i.e. 2D processes which are likely distorted by the 3D effect. Another limitation is the possibility of some errors in integral scale estimates due to the so called "crossing trajectories" effect in which trajectories of fluids and trajectories of finite particle separate. This cross trajectory effect also leads to clustering of particles into non-vortical region [13]. These effects are caused by the finite size of particles and drag effect. Surface drifters also act as filters and thus limit the size of eddies that can be captured to those with similar scales and greater. While significant efforts with laboratory experiments and Direct Numerical Simulations (DNS) are being made to correct for these effects in models [14], correction in environmental flows is still an area of an on-going research because of the difficulty in obtaining true Lagrangian data in open flows [13].

Dispersion of particles can be studied by means of single dispersion analysis and multi-particle dispersion [15]. Single particle statistic or absolute diffusion is the first order estimate of diffusion which exhibits generic tendencies of quadratic initial evolution and linear evolution at time scale significantly larger than the Lagrangian time scale [16]. The theory follows Taylor's diffusion by continuous movement [17] and the detailed formulation of Lagrangian statistics are documented in the work [15]. The key parameters for diffusivity estimate from the method lie in the determination of the Lagrangian autocorrelation function which determines the length and time scales of eddies responsible for mixing at the scales of interest. These two key parameters are also inputs for modelling mixing caused by turbulent eddies and are therefore required for a valid Lagrangian description.

This research aims to study the spatio-temporal variation of velocity and dispersion in typical shallow water estuaries to underpin the current modelling efforts in shallow waters.
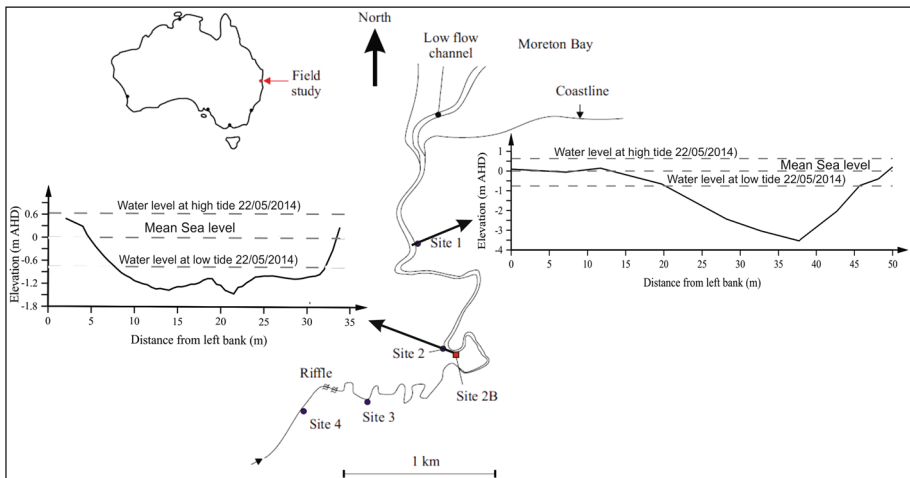

Fig. 1 Eprapah Creek estuarine zone, including surveyed cross sections on 29 Sept. 2013; the cross sectional average depth at mean sea level for site 1 and site 2 are 1.31 and 0.42 m, respectively. Mean sea and water levels at high and low tides on 22 May, 2014 are indicated on cross sections

This paper presents the single dispersion analysis of the high resolution drifter observation at scales less than a tidal period. At this scale, the Lagrangian integral and length scale is about 20 s and 20 cm, respectively. The estimate of diffusivity is from velocity autocorrelation functions based on time series 600 s long and satisfies the long term criterion amongst others. In addition, the study focused on three major concerns with diffusivity in tidal shallow water at tidal time scales less than a tidal period; (1) temporal variability of integral scales and horizontal diffusivity, (2) the effect of large velocity fluctuations (horizontal shear) on the scales of apparent diffusivity in a tidal shallow water and (3) consistency of scaling of diffusivity with relevant length and time scales.

2 Field experiment

Eprapah Creek consists of fairly straight and meandering channels (Fig. 1). The channel is characterized by variable channel cross sectional area, sinuosity and irregular bathymetry. The estuarine zone extends to about 3.8 km from the mouth of the estuary and has a maximum depth between 3 and 4 m mid-estuary and reasonably sheltered from wind by overhanging mangroves [18].

Bathymetric surveys of the channel were conducted on the 29 and 30th of September 2013 at Australian Mean Thread Datum, AMTD 0.3 km (site 1), AMTD 2.0 km (downstream site 2B), AMTD 2.1 km (site 2B) and AMTD 3.0 km (site 3). The cross-sections were asymmetrical, deeper towards the right bank in an ebb flow direction and widen toward the mouth. Between the mouth and the upper estuary, the channel maximum depth varied from 1 to 3.5 m below the mean sea level. The bathymetric survey revealed a
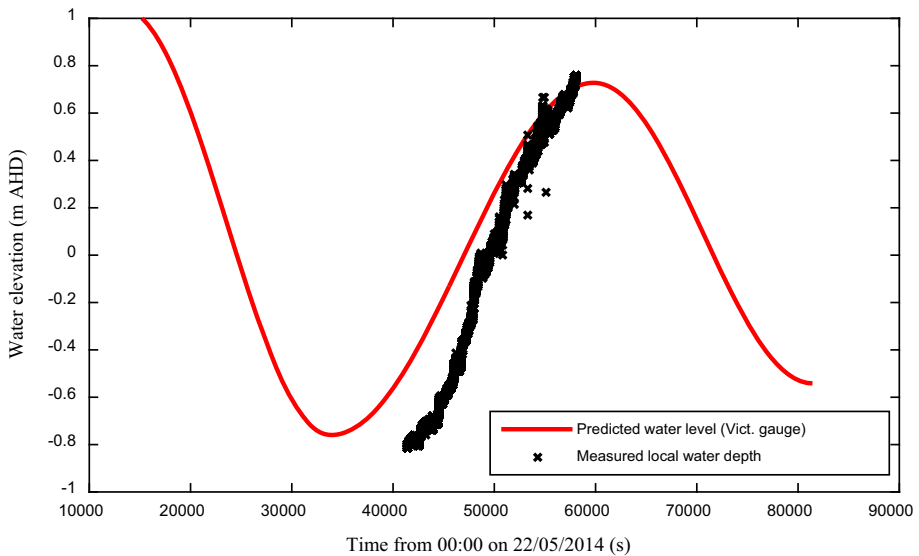
Fig. 2 Water level prediction in meters Australian Height Datum (m AHD) at Victoria point gage (27°35′S 153°19′E) (data: Bureau of Meteorology, BOM) and the local water level observed as averaged height observed by three high resolution drifters. Time measured in seconds from 00:00 on 22/05/2014 Australian Eastern Standard Time (+10 UTC)

reduction in cross-sections from the mouth through the upper estuary. The cross-section area, A, decays exponentially along the length from the river mouth:

$$A = A_o \exp\left(-\frac{x}{a}\right), \tag{1}$$

where A_o is the cross-sectional area at the mouth, x is the longitudinal distance from the mouth and a is the convergence length [19]. The detailed analysis of the survey data alongside 4 other transects obtained between AMTD 1–2 km on the 31st of August 2013 yielded $A_o = 106$ m^2 and a = 1.4 km at mean sea level [18]. The cross sectional average depth at mean sea level for site 1 and site 2 are 1.31 and 0.42 m, respectively.

A Lagrangian drifter experiment was carried out on May 22, 2014 at Eprapah Creek, Australia, a site where a series of Eulerian studies [20, 21] and Lagrangian studies [18, 22] have been previously undertaken. The drifter experiment was carried out during a flood tide with tidal range of 1.4 m (Fig. 2). Figure 2 shows the comparison between the predicted water level at Victoria Point gage, about 3.5 km away from the mouth of the estuary and local water level measured by high resolution drifters. Some disparity in the water level particularly at the beginning of the experiment is related to differences in water level between the channel and Moreton Bay and some phase lag in the channel response to tidal forcing. An average wind of 1.1 m/s from the North–North–East direction over the period of the experiment was recorded. The surface waves resulting from wind alignment along banks were calm with low amplitude and period about 0.5 s. Therefore, the influence of wave rectification on the drifters was presumably insignificant. Table 1 summarises the conditions of the field during the experiment.

A fleet of 3 GPS-tracked drifters was deployed at the mouth of the creek during the flood tide. Logistical and financial constraints limited the number of drifters to 3. However, the analysis technique described in Sect. 3.4 presents a method of segmentation of drifter trajectories which enables the effective number of drifters to be increased an order of magnitude. The explanation includes a sensitivity analysis to ensure this approach does not bias the estimate of autocorrelation function or associated parameters. The drifters, of a high resolution design described in [12], were sampled at 10 Hz and have position accuracy in the order of 2 cm, thanks to the GPS real time kinematic (RTK) processing technique [23]. The drifters were designed as a waterproof cylindrical capsule diameter 19.7 cm and height of 26 cm with less than 3 cm of the total height unsubmerged in water to allow satellite communication for fixed GPS solution. The wind slip estimate, based on the bulk wind data and the average speed of the drifters, was about 0.007 m/s, i.e. less than 1 % of the wind speed [12]. Because the drifters are positively buoyant, they are not

Table 1 Overview of the environmental conditions of the field during experiment

Conditions	Details
Tidal condition	Flood neap tide; Tidal range = 1.4 m
Boundary condition	Mean water depth = 1.96 m (site 1) and 1.07 (site 2) Width at MSL ∼50 m (site 1) and ∼30 m (site 2)
Hydrologic condition	Total of 40 mm rainfall within 30 day prior to experiment
Atmospheric condition	Calm with average wind speed ∼1.1 m/s from NNE; moderately humid, air temperature between 18 and 24 °C

subjected to vertical shear dispersion. However, the design is stable in water and thus water level was estimated to an accuracy of about 2 cm. The drifters were deployed at the same time at the centre of the channel in a straight line with each separated by at least 60 cm. This separation avoided collision between drifters and reduced the interference of other drifter particles on motion of each drifter particular during the initial drift stage. The deployments lasted for a 4-h period, and the drifters were monitored from canoes at a minimum distance of 20 m downstream of the flow to avoid interference with the drifters.

3 Data analysis

3.1 Quality control

Data processing involved removal of spurious data, filtering and coordinate transformation. The raw GPS position data achieved 92 % of the fixed solution ($\pm$1 cm) with only 8 % of a float solution ($\pm$10 cm) for all three drifters. Degraded GPS solutions and external disturbances were found to be associated with acceleration greater 1.5 m/s^2 [12] while peak tidal flow in Eprapah Creek is about 0.3 m/s [24]. Therefore, the data were de-spiked such that points resulting in velocity greater than 0.6 m/s (i.e. twice the largest expected peak flow velocity) and acceleration greater than 1.5 m/s^2 were removed and flagged using quality control algorithms developed in MATLAB. The spikes are anomalies of GPS/RTK solutions due to challenging observation conditions from sheltered mangroves and presence of extreme end of float solution during limited satellite constellation. The spikes in residual velocity data were additionally identified by Phase-Spaced Thresholding as those lying outside the universal threshold range defined by an ellipsoid of 3D Poincare phase space [25]. The process resulted in removal of no more than 8 % of samples in the position time series. Gaps less than 10 s were filled using a spline interpolation [26], while gaps between 10 and 20 s were reconstructed using a linear interpolation. A gap larger than 20 s was simply removed by splitting a trajectory into two separate short ones. The Savitzky–Golay low-pass filter [27] was applied on the position time series to remove the high noise content that dominated the spectra at high frequency with cut-off frequency $F_c > 1$ Hz without distorting the underlying signal.

3.2 Coordinate transformation

Tidal open channel flows have strong directional preference. The mean flow is stronger in the streamwise direction than the cross shore direction because tidal incursion and excursion force the flow along the stream. Because of this anisotropy and limited width of Eprapah Creek, the proper description is the channel based moving coordinate [12]. The position time series were transformed from a local geodetic East–North–Up, e–n–u coordinate to a channel based Streamwise–Cross stream–Up, s–n–u coordinate using the method described in [28] which requires the coordinates of the channel centreline. Herein, 's' represents the streamwise direction +ve in the downstream, n is cross stream direction, +ve to left, while 'u' is +ve in the upward direction. The 'u' values are finally transformed to Australia Height Datum (m AHD) and averaged in time over for all drifters for evaluation of the dependence of diffusivity on the tidal phase.
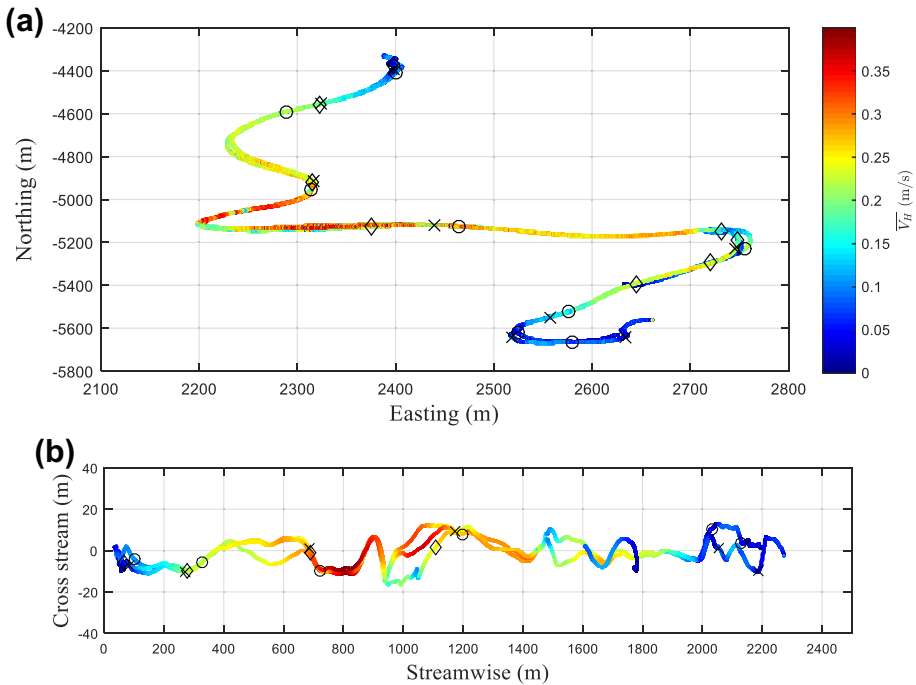
3.3 Field drifter trajectories

Figure 3a shows the trajectories of the drifters, coloured by the time-averaged mean horizontal velocity, $\overline{V}_H$, is estimated using a moving window time averaging technique with a window size of 200 s in an interval of 1 s as follows:

$$\overline{V}_H = \sqrt{\overline{V}_s^2 + \overline{V}_n^2}. \tag{2}$$

The window size is chosen in line with Trevethan et al. [20] who calculated turbulence statistics over 200 s.

Upon deployment, two of the drifters made 1–3 loops about 3 m in diameter as they were trapped in the inlet vortices before drifting toward the river through the flood channel. The drifters followed the outer part of the estuary in an effect caused by high tidal momentum. The mean flow showed strong tidal dependence and the velocity maxima occurred after a low tide (Fig. 3a), i.e. about 1 h after deployment. This velocity-stage phase was consistent with previous Eulerian observations within the channel [29]. Figure 3b shows the same spatio-temporal plot of the mean velocity presented in Fig. 3a but projected in the channel based coordinate. The $\overline{V}_H$ data were not affected by this transformation. The mean streamwise velocity magnitude, $\overline{V}_s$, was typically about 5 times larger than the corresponding the cross stream velocity, $\overline{V}_n$ except at the meanders. At the

Fig. 3 Drifter trajectories coloured by the mean horizontal velocity, $\overline{V}_H$ (m/s) in: **a** e–n–u coordinates; **b** s–n–u coordinate. About 4.5 h long data set during the neap flood tide on 22/05/2015. *Symbols* are placed at an interval of 30 min; drifter 1(*open circle*), drifter 2 (*open diamond*) separated into two trajectories; drifter 3 (*cross symbol*)

meanders, the tide forced the drifters toward the outer radius where a magnitude of $\overline{V}_n$ rose significantly to match the corresponding $\overline{V}_s$. The drifters captured the mean velocity fluctuations accurately (i.e. large scale fluctuations including tide and external resonances), because the length scale of their evolution is larger than the length scale of the position uncertainty of the GPS-tracked drifters [12].

The position uncertainty has been observed to indicate a local dispersion regime in the neighbourhood of the length scale of the noise [30] and could lead to spurious residual velocity statistics. Hence, the position time series were further subsampled to 1 Hz before obtaining residual velocities and their derivatives.

3.4 Single particle statistics

Single particle analysis (absolute dispersion) involves the statistics of the behaviour of a parcel of fluid as it evolves in a fluid domain with respect to a fixed point. This can be used to predict the location of particles and scalars at various times [15]. Absolute dispersion, D, is the mean-squared separation of particles from their initial position at a given time. For a large number of realizations of N Lagrangian drifter trajectories:

$$D(t) = \frac{1}{N} \sum_{n=1}^{N} \left[X_i^n(t) - X_i^n(t=0) \right]^2, \tag{3}$$

where X is the position of drifter n in the i-direction (i = s or n) and t is the time from release. The estimate in Eq. (3) provides means for examining the various dispersion regimes. The time derivative of D(t) provides a measure of absolute diffusivity which reflects the spread and the drift of independent trajectories from a source point. Because of unsteadiness in a tidal system, a large number of concurrently sampled drifter trajectories would be required to obtain this estimate. Segmentation of a drifter track observed at a time less than a tidal cycle fails because drifter motion contains unsteady, non-stationary tidal drift and drift associated with residual velocity. An alternative approach to estimate the scale of diffusivity caused by the residual velocity is from the integral of velocity auto-correlation function obtained from stationary residual velocity [15, 31]. The basic theory behind single particle analysis as described by Taylor [17] is based on the assumptions that the flow field is homogeneous and stationary. Herein, integral scales and the scales of eddy diffusivity are obtained from the analysis of residual velocity.

3.4.1 Lagrangian integral scales and diffusivities

The integral length scale describes the size scale of eddies responsible for turbulent mixing. It can be estimated as:

$$L_{Li} = \left(\langle v_i^2 \rangle_L \right)^{1/2} \times T_{Li}. \tag{4}$$

The Lagrangian integral time, T_L sometimes referred to as the decorrelation time scale, is the time over which Lagrangian velocity could be considered correlated with itself. It is considered the basic indicator of Lagrangian predictability [15]. T_L is estimated as the integral of Lagrangian velocity autocorrelation function R_L such that [32]:

$$T_{Li} = \int_0^\infty R_{Li}(\tau). \tag{5}$$

The autocorrelation function is the normalised covariance of the Lagrangian velocity, which contains the memory of the drifters. It is computed at each time lag τ as an ensemble of trajectories or short realisations for the 'i' velocity component using:

$$R_{Li}(\tau) = \frac{\int_0^T (v_i'(t)v_i'(t+\tau))dt}{\langle v_i'^2 \rangle_L}, \tag{6}$$

$$v_i(t) = V_i(t) - \overline{V_i}(t), \tag{7}$$

$$\overline{V_i}(t) = \frac{1}{\Delta T} \int_i^{i+\Delta T} V_i(t)\, dt. \tag{8}$$

The distribution of residual velocity, v_i in Eq. (7), is sensitive to the method by which the mean velocity, $\overline{V_i}$, is removed from the instantaneous velocity, V_i. The three standard approaches for estimating the mean velocity in ocean drifter studies are: (1) spatially binned (Eulerian) velocity field; (2) the use of constant velocity equivalent to length of drifter study; and (3) spline estimate [15]. The spatial binning approach requires some prior knowledge of the decorrelation time scale for the scale of fluctuation under consideration and it introduces additional uncertainty such as the selection of size of bin for the velocity vector field and unsteadiness of tidal scale velocity within the channel. The use of a constant mean assumes the underlying drift is linear. Applying this method to this data set resulted in a decorrelation time scale that was larger than the scale of interest, particularly in the streamwise direction. This is because unsteady continuous tidal signals and resonance is not removed from the residual velocity [33]. Herein, by ignoring the inhomogeneity in the flow, the residual velocities were obtained by removing the time varying mean, $\overline{V_i}(t)$, from the individual drifter trajectories using Eq. (4). $\overline{V_i}$ is obtained by applying a moving window time averaging technique with window size $\Delta T = 200$ s in an interval of 1 s. The averaging procedure assumes that there is a gap in the velocity frequency spectrum which does not exist for the present observation. It will be shown later that the decorrelation time scale is less than 40 s. The time $T = 200$ s ensured that the estimate of $\overline{V_i}$ has more than 5 degrees of freedom. Therefore, the statistics of the resulting residual velocity were considered stable. In addition, $T = 200$ s was similarly obtained from a sensitivity analysis on ADV data for extracting turbulent velocity from instantaneous velocity in previous studies at Eprapah Creek [21].

The scales of eddy diffusivity for the streamwise and across stream are obtained from the autocorrelation function as:

$$K_{ii} = 2\langle v_i^2 \rangle_L \int_0^\infty R_{Li}(\tau)\, d\tau, \tag{9}$$

The presence of low frequency motions often results in an autocorrelation function which fluctuates with negative lobes covering a large area, introducing large error to the estimate of T_L. Therefore, the integration is performed up to the time of the first zero crossing [32]. Only 3 drifter trajectories are available from the field deployment. However, the estimates of R_L, T_L and K require a large number of trajectories with sufficiently long realisation length, T_R. In order to maximise the use of a limited number of trajectories, it is common to split long trajectories into non-overlapping segments with duration T_R [34]. The choice of period T_R is important because it has to be long enough to accurately consider long time velocity correlation and short enough to avoid altering of the

Lagrangian mean velocity. T_L values were first calculated from the residual velocity of the 4 independent trajectories (Table 2). The values of T_L obtained by separately integrating the ensemble autocorrelation functions for the streamwise and the cross stream are 19 and 21 s, respectively. The time of zero crossing for R_L is about 60 s, which implies that the number of uncorrelated samples for an overall observation length of 46,128 s is about 760 (Table 2). The method of segmentation is therefore applied, taking advantage of redundant uncorrelated data. Effect of T_R and consequently, the number of realisation on R_L and T_L was examined (not shown). Varying T_R between 2000 and 440 s resulted in an increase in number of realisation from 25 to 100. Despite this increase in the number of realisations, R_L showed no significant change particularly before zero-crossing while the mean value of T_L was stable [18]. Herein, $T_R = 600$ s was chosen that fulfils the Nyquist principle to avoid aliasing in signal with period of 200 s and sufficiently long enough to affix diffusivity to the velocities fluctuations. This resulted into 75 non-overlapping realisations from which estimates of R_L, T_L L_L and K presented in Sect. 4 are made. Refer to Suara et al. [18] for more detail on this selection.

3.5 Fixed drifter measurement analysis

The magnitudes of T_L L_L and K associated with inherent errors due to GPS position fixing and hardware noise is examined. Assuming the GPS position fixing is independent of drifter motion and location, measurement taken at a fixed location is representative of the inherent errors [12]. Position time series from the fixed drifters described in Suara et al. [12] were quality controlled, low-pass filtered with cut-off frequency, Fc = 1 Hz and analysed using relevant equations in Sect. 3.4. The standard deviations of residual velocities, v_i and T_L obtained from the fixed drifter are an order of magnitude higher than those from the field measurements. Therefore, the magnitude of L_L and K_L associated with inherent errors are at least 2 orders of magnitude less than those presented in Sect. 4.

4 Results and discussion

4.1 Basic flow observation and Lagrangian velocity spectra

Figure 3 shows the trajectories of the drifters both in local geodetic and channel based coordinates, coloured by the time averaged $\overline{V}_H$. Maximum velocities of about 0.3 m/s

**Table 2** Statistical distribution of residual velocity, v_i, obtained from Eq. (6) [18]

Track ID	Drift duration (s)	Streamwise component (v_s)				Cross stream (v_n)			
		$\overline{v}_s$ (m/s)	Std (v_s) (m/s)	Sk (v_n)	Ku (v_n)	$\overline{v}_n$ (m/s)	Std (v_n) (m/s)	Sk (v_n)	Ku (v_n)
1	16,601	0.00099	0.0064	−0.120	3.7	0.00076	0.0060	−0.180	4.0
2a	8451	0.00130	0.0085	0.096	4.6	0.00110	0.0100	0.060	3.5
2b	4639	0.00006	0.0027	−0.240	3.4	0.00003	0.0023	−0.140	5.8
3	16,437	0.00026	0.0110	0.190	9.6	0.00079	0.0059	−0.035	4.0
Overall	46,128	0.00070	0.0084	0.11	10.9	0.00077	0.0067	0.052	7.5

occurred during the earlier part of the flood, similar to observations made with using acoustic Doppler velocmeters, ADV [29]. After 4 h, the drifters slowed down to a velocity less than 0.1 m/s at a distance of about 2 km from the mouth. This was toward the end the flood tide.

Motion of particles in a turbulent flow occurs over a broad range of length and time scale. The Eulerian velocity spectra and the statistics of 'true' turbulence within Eprapah Creek have been observed to have structure associated with existing turbulence theory and similar to the classical boundary layer observations [29]. To verify that the drifter motion within the period of observation was driven by this underlying turbulence, the instantaneous velocity spectra for the raw and post processed data were examined. Figure 4 shows some power spectra of instantaneous velocities average for the 4 independent trajectories. The power spectral densities of velocities between 0.0001 and 0.5 Hz were well fitted with slope of 5/3 predicted by the Kolmogorov similarity hypothesis within the inertial subrange [35] and were similar to the Eulerian power spectrum [29].

The Lagrangian velocity spectra showed energetic events across the frequency range, with some distinctive troughs and peaks in the range 0.001 and 0.1 Hz which were related to turbulence fluctuations due to internal resonances. The velocity spectra did not show signs of saturation of energy density toward the low frequency when compared with the spectra of ADV velocity data collected over a period of two tidal cycles [29]. This seems to be a result of the presence of low frequency fluctuations such as external resonance, which were not completely resolved due to the short length of the drifter study. The raw data spectra showed presence of noise at frequency large 1 Hz while the post processed data showed the true turbulent velocity spectra without the high frequency noise content.

The largest scales present in the drifter velocity distribution were obtained by the ensemble average, R_L, for the residual velocity after removing the constant overall mean based on the 4 separate trajectories. This resulted in an integral time scale of about 2 orders of magnitude, and about 4 times the values obtained, respectively for streamwise and cross
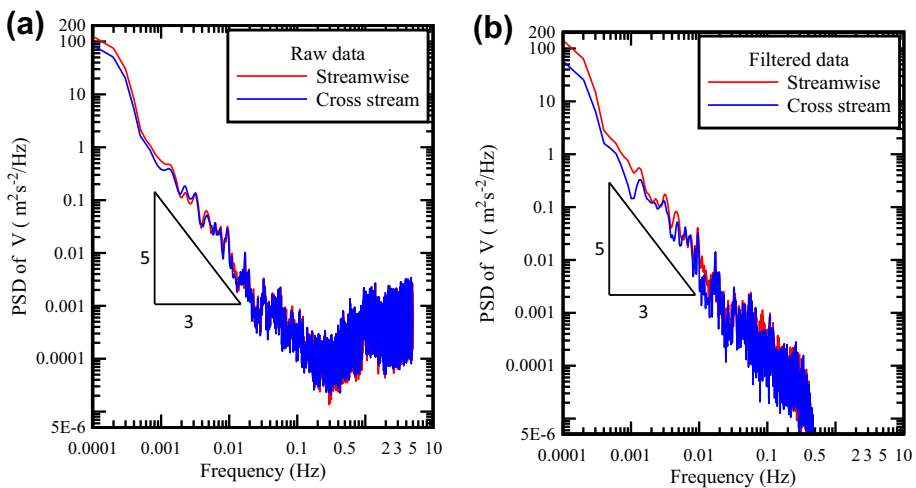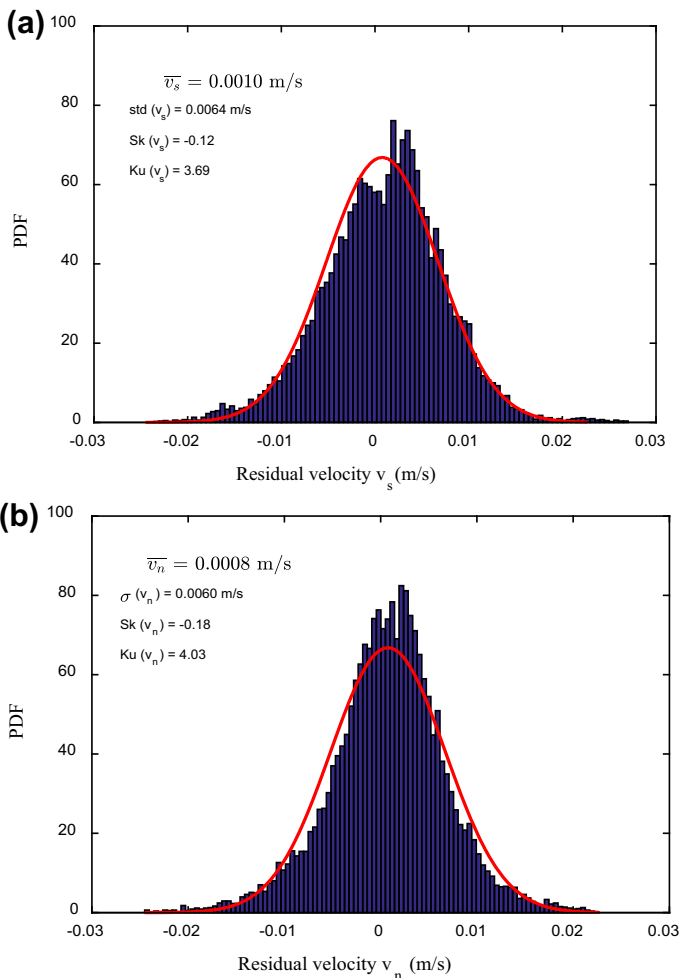

Fig. 4 Average PSD of instantaneous velocities using 4 independent trajectories with 50 % overlapping providing 8 degrees of freedom: **a** raw transformed data sampled at 10 Hz; **b** filtered data, down-sampled to 1 Hz. Kolmogorov similarity hypothesis shown in *black triangle*

stream components using the residual velocity obtained from a running mean of window
T = 200 s.

4.2 Residual velocity distribution

Table 2 summarises the statistical distribution of the residual velocities from the 3 drifters.
The mean residual velocities ($\overline{v}_s$, $\overline{v}_n$), are close to zero, while the standard deviation (std)
for both the streamwise and cross stream direction was about 0.01 m/s. Figure 5 shows the
streamwise and cross stream residual velocity distribution for track 1 (Table 2) overlaid
with the probability distribution function, PDF of an equivalent Gaussian distribution. The
skewness and kurtosis herein are normalized by the standard deviation and are equivalent

(a)

$\overline{v_s} = 0.0010$ m/s

std (v_s) = 0.0064 m/s

Sk (v_s) = -0.12

Ku (v_s) = 3.69

PDF

Residual velocity v_s (m/s)

(b)

$\overline{v_n} = 0.0008$ m/s

σ (v_n) = 0.0060 m/s

Sk (v_n) = -0.18

Ku (v_n) = 4.03

PDF

Residual velocity v_n (m/s)

Fig. 5 Distribution of residual Lagrangian residual velocity for drifter 1: **a** streamwise component **b** across
stream component. Overlay in *red* is a PDF of Gaussian distribution of equivalent size as the residual
velocity with mean and standard deviation of 0 and 1, respectively

to 0 and 3, respectively, for the Gaussian distribution. The skewnesses (Sk) were close to zero with the cross stream distribution closer to Gaussian distribution than that of the streamwise.

The kurtoses (Ku) were slightly larger than the value of 3 (i.e. value expected of a Gaussian distribution). This resulted from the flatness of the distribution tails owing to some instances of large amplitudes of fluctuation extending beyond the above the normal distribution curves along the histograms tail (Fig. 4). This might be linked to some degree of inhomogeneity and the intermittency of the turbulence field. The large kurtosis values were indicative of the large distribution size, while smaller values were observed for local temporal distribution. The results showed that the statistics of the residual velocity distribution were not significantly deviated from Gaussian distribution. This result suggests that the dispersion within the system at time scale less than a tidal period can be modelled using a Lagrangian stochastic model (LSM) with the accurate information of the spatio-temporal variation of the standard deviations and the integral scales.

4.3 Lagrangian integral scales and scales of diffusivity

Figure 6 shows the R_L curves for the streamwise and cross stream components using non-overlapping segments with $T_R = 600$ s resulting into 75 independent realizations. The values of T_L obtained by separately integrating the R_L curves are $T_{Ls} = 18 \pm 8.7$ s and $T_{Ln} = 20 \pm 8.4$ s, streamwise and cross stream, respectively. The integral time scales obtained over the length of the estuarine zone have similar magnitude to the values $T_{Ln} = 15$ s and $T_{Ls} = 50$ s previously obtained for a straight section of Eprapah Creek [12]. The length scale estimate as $L_{Ls} = 0.18 \pm 0.09$ m and $L_{Ls} = 0.14 \pm 0.05$ m in the streamwise and cross stream components, respectively. These values are of the same order of magnitude with the mixing length scale estimate $L \sim 1$ m reported in [36].
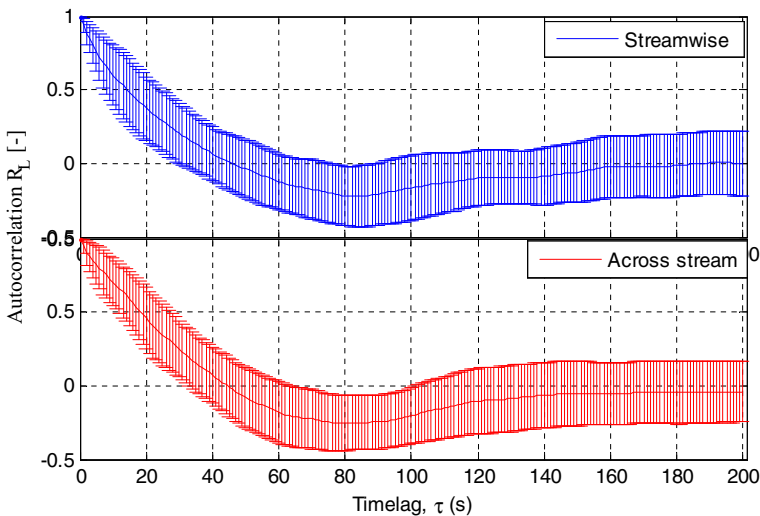
Fig. 6 Lagrangian autocorrelation function for streamwise and cross stream components obtained from ensemble of 75 non-overlapping realisations with length, $T = 600$ s

In order to evaluate the variability of the integral scales with different phase of the tide, calculations [Eqs. (4) and (5)] were carried out over short windows of 3280 s for the 75 non-overlapping realisations. This window size was chosen such that the number of resulting data sets covered the different major stages during the flood tide and to have a significant numbers of realisations. This resulted in 5 data sets (i.e. 2 estimates each below and above mean sea level, MSL i.e. water elevation $\sim$ zero, and 1 at about MSL) with 15 realisations per window. Table 3 summarises the distributions of the integral scale streamwise and cross stream components with the phase of the tide. The distributions revealed integral time scale that varied between 16–28 s and the integral length scales between 0.10–0.62 m. The results showed some dependence of the integral scales on water depth and mean velocity. Although, factors such as slope of the channel, meanders affect the integral scales, T_{Ls} was largest at about MSL. The length and time scales were largest at peak of the tidal inflow. This time corresponded to the time the drifter approached the meanders which is about 800 m from the mouth of the channel. The mean integral scales were well correlated with mean flow velocity. This suggests the turnover time of eddies varied more in time than in space during the flood tide. The integral time scales were about 2 orders of magnitude larger than the Eulerian integral time scales obtained near the channel bed [37]. While ejection and sweep processes of tidal forcing against channel bed predominated the mixing within the channel boundary layers large scale processes such as wind vertical shear and lateral shear contributed to the size of the eddies in the sub-surface layer.

The diffusivity scale of $K_{ss} = 0.0025 \pm 0.0012$ m^2/s and $K_{nn} = 0.0012 \pm 0.0005$ m^2/s were obtained from the stationary turbulent residual velocity. These values were in the same order of magnitude with the minimum lateral dispersion coefficient, $K_{nn} = 0.003$–0.42 m^2/s obtained from dye tracer studies particularly in similar shallow sites (depth <5 m) such as Cardiff Bay, Loch Ryan, Forth Estuary, Humber Estuary in the United Kingdom and Saone in France [5]. The values $K_{ss} = 0.0025 \pm 0.0012$ m^2/s and $K_{nn} = 0.0012 \pm 0.0005$ m^2/s were smaller than the values ($K_{ss} = 0.57$ m^2/s and $K_{nn} = 0.053$ m^2/s) estimated from the relatively larger scale dispersion resulting from interaction of tidal current and unsteady external resonance [12]. Eddy viscosity, a vertical mixing parameter was previously observed in Eprapah Creek to vary between 10^{-5}–10^{-2} m^2/s next to the bed within a tidal [37]. The diffusivity data obtained from the surface drifters are 1 to 2 orders of magnitudes larger the values of turbulent eddy viscosity obtained close to the bed. This suggests the contribution of large scale processes to mixing close to the surface compared to next to the bed where mixing is mainly caused by small

Table 3 Variation of integral time and length scale with tidal phase

Time (s)	Water elevation (mAHD)	H (m)	Lagrangian time scale		Lagrangian length scale	
			T_{Ls} (s)	T_{Ln} (s)	L_{Ls} (m)	L_{Ln} (m)
41,590–44,870	-0.74 ± 0.04	0.56 ± 0.04	17 ± 7.1	16 ± 6.8	0.21 ± 0.10	0.13 ± 0.06
44,871–48,150	-0.47 ± 0.10	0.83 ± 0.10	17 ± 6.8	28 ± 5.8	0.44 ± 0.20	0.62 ± 0.10
48,151–51,430	-0.013 ± 0.10	1.30 ± 0.10	20 ± 6.0	20 ± 10	0.42 ± 0.10	0.43 ± 0.20
51,431–54,710	0.33 ± 0.10	1.60 ± 0.10	19 ± 7.3	19 ± 7.3	0.16 ± 0.06	0.12 ± 0.05
54,711–57,990	0.56 ± 0.05	1.90 ± 0.05	17 ± 9.2	20 ± 7.1	0.08 ± 0.04	0.04 ± 0.03

Time measured in seconds from 00:00 on 22/05/2014 Australian Eastern Standard Time (+10 UTC). Depth H is estimated as the water elevation above MSL observed by the drifter, time averaged over the three drifters and added to the average channel depth across site 1 at MSL

scale processes and bed induced turbulence. A possible explanation for large variation in the magnitude of the mixing parameters within a tidal cycle could be the additive nature of scales of processes resulting in the velocity fluctuation within the channel. This occurs such that the dominant process varies with tidal phase. This suggests that orders of magnitudes variation in mixing parameters is an important feature of small channels and needs to be accounted for in accurate modelling of tidal mixing in such similar water bodies.

To examine the variability of the scale of the Lagrangian diffusivity with the phase of the tide, estimates were made over a small time window as employed for the integral scales. Figure 7 shows the distribution of diffusivity with the water elevation measured by the drifters and averaged in time. The estimated diffusivity varied between 0.001–0.02 m^2/s during the experiment. Peak diffusivity was observed at the early part of the flood which corresponds to the peak horizontal mean velocity. A linear correlation ($R^2 > 0.9$) between with horizontal velocity, V_H and the diffusivities was observed (not shown). This suggests the diffusivity in models can be scaled by the mean horizontal distribution in this flow.

For comparison, a dimensionless diffusivity, K, is defined as:

$$K = \frac{K_{eff}}{V_{rep} \times H}, \tag{10}$$

where K_{eff} is the effective diffusivity/dispersion coefficient, V_{rep} is a representative velocity and H is a representative depth. The dimensionless effective diffusivities from the present study are compared with values from dye experiments for various English channels [5] and drifter experiments at tidal inlet New River Inlet, North Carolina [11]. The effective diffusivities in the present study are average of the diffusivities $\left(\frac{K_{ss}+K_{nn}}{2}\right)$ (Fig. 7) normalised with corresponding averaged horizontal velocities and depths, H (Table 3). The dye experimental data are minimum lateral dispersion coefficients reported for the channels and are normalised with the corresponding tidal currents and depths provided. Spydell et al. [11] data are clustered drifters spreading rates which are normalised the averaged
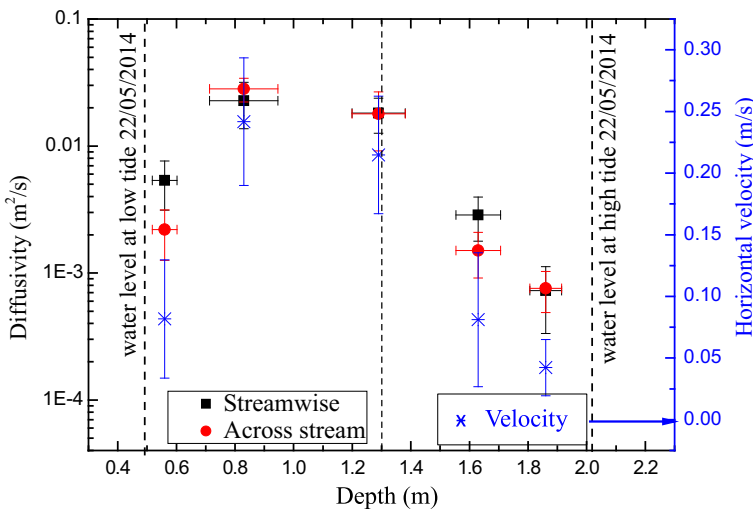

Fig. 7 Lagrangian diffusivity and averaged horizontal velocity (Eq. 1) as a function of depth at site 1 for the present experiment only. Note that the diffusivity (*left vertical*) is in logarithmic scale. Depth, H is estimated as the water elevation observed by the drifter, time averaged over the three drifters and added to average channel depth across site 1 at MSL; *Error bars* extending to ±1 SD

centroid velocities of the clusters and averaged depths for inside and outside the channel. K values in the present study varied between 0.02 and 0.11 which is within the range of 0.005–7 [5] obtained from the dye experimental data and smaller than the drifter spreading data values of ~ 0.13 and ~ 0.22 in and outside the tidal channel, respectively [11]. The larger values are indicative of mixing cause by large scale dispersions. While the results from the combination of the these experimental data do not show a discernible trend with the velocity, K values in the present study shows that diffusivity increased with the increase in the tidal horizontal velocity (Fig. 8).

4.4 Effect of long oscillation and scaling of diffusivity

Having calculated the diffusivity from residual velocity by scale separation using a moving average with $\Delta T = 200$ s, discussing the effect of horizontal shear on the scale of diffusivity is important. It is worth emphasising that the horizontal velocity distribution in the tidal channel is also caused by interaction of tidal flow and resonance with the boundary geometries such as mangroves, banks, meanders and channel bed. This induces some horizontal shear velocity distributions which could inherently cause rapid increase in the horizontal diffusivity estimates. To support this conjecture, the effect of ΔT on the scale of diffusivity is examined. The diffusivity is this section is assigned an apparent diffusivity because of inclusion of shear dispersion for large values of ΔT. Figure 9 shows that the apparent diffusivity increased by two orders of magnitude of ΔT between 100 and 800 s. This suggests that horizontal shear could be an important indicator for mixing in small tidal shallow estuaries particularly at scale less than a tidal period. The across stream diffusivity tended to an asymptotic value of 0.01 m^2/s with ΔT about 600 s suggesting an upper limit of lateral mixing.
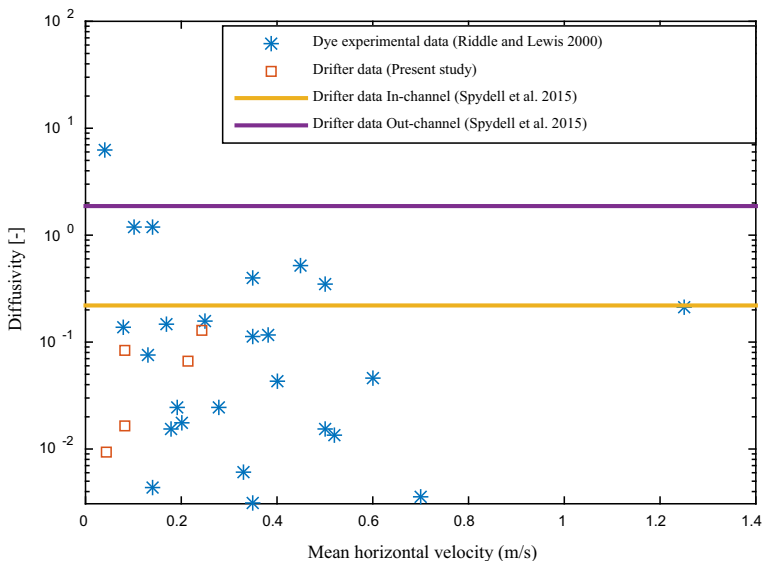

Fig. 8 Dimensionless effective diffusivity as a function averaged horizontal velocity in square; Dye experimental data are dimensionless lateral dispersion data (i.e. normalised with tidal current and depth) from in various English channels (Table 1, in [5]) and drifter experiment and the drifter data are cluster spreading rates normalised with cluster centroid velocities and depth in a tidal inlet [11]
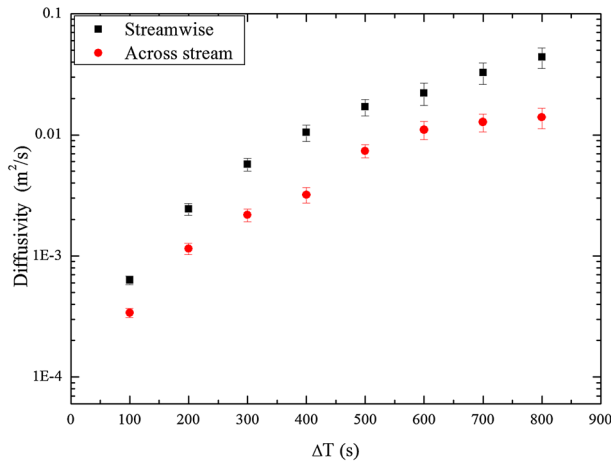
Fig. 9 Effect of ΔT on the scale of diffusivity over taken through the data set. Note that the number of realization varied between 152 for ΔT = 100 s and 16 for ΔT = 800 s; *Error bars* extending to ±1 SD

Fig. 10 Apparent diffusivity against the length scale; Okubo's ocean diffusion data from dye experiments [2], Okubo's length scale of diffusion is defined as 3 times the radius of radially symmetrical dye distribution. Thick slant lines represents the 4/3 power fit and dash line represent local 4/3 power fit [38]
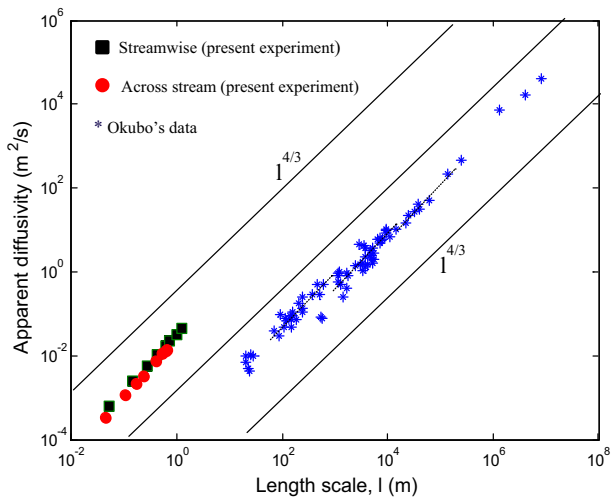
For comparison and to examine the similarity between the scaling of small scale mixing parameters with the channel and existing bodies of theory, the plot of the apparent diffusivity against the length scale of diffusion are presented alongside with Okubo's dye experiments ocean diagram data in Fig. 10. Okubo [2] data were obtained from the dye tracer diffusion experiments covering the time scale ranging from 2 h to 1 month and length scale ranging from 30 m to 100 km from subsurface layer of the sea. Despite the difference in geometry, physics of the systems, approach and method of estimates, it is clearly observed in Fig. 10 that the diffusivities scale locally by 4/3 Richardson power law scaling for prediction of spreading in oceanic and atmospheric turbulence [2, 38]. Note that the Lagrangian integral length scale is used herein to represent the relevant length scale. This is expected to be smaller than the length scale of a dye plume and therefore partly

Fig. 11 Average PSD of residual streamwise velocity showing decrease in turbulence energy dissipation rate with the increasing period ΔT used as filter for extracting scales of interest
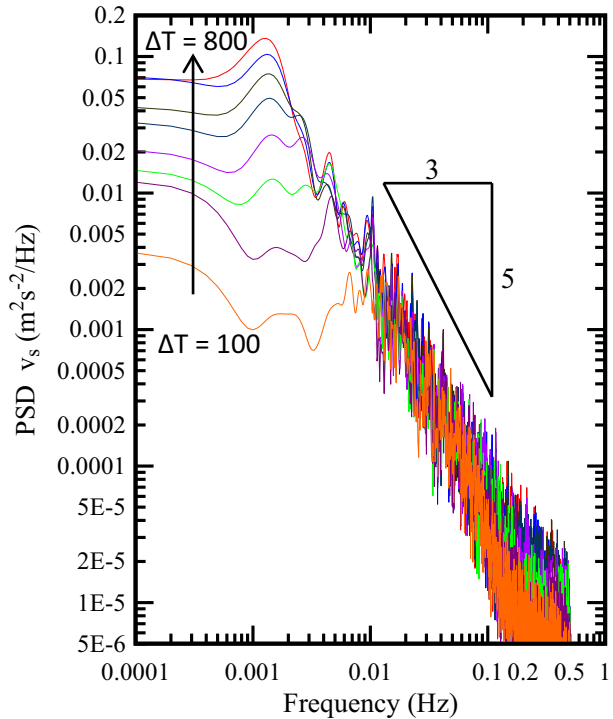
explains why the diffusivity estimates here are farther to the left. The scaling is consistent from the $-5/3$ power law because the rate of turbulent energy dissipation varied with different time scale and the scaling is independent of the ΔT as shown in Fig. 11. Consistently, the estimated Lagrangian integral length scale i.e. scaling for square root of variance of a water patch, obtained by varying ΔT varied as 3/2 power of the Lagrangian integral time scale (not shown). This is similar to the third power law scaling of variance of dye patch with the diffusion time observed form oceanic diffusion [2]. Modelling of small scale mixing within tidal shallow estuaries can therefore be approached with classical scaling analysis upon identifying pertinent parameters. However, the diffusivity estimates are orders of magnitudes lower than many existing data set.

5 Conclusions

High resolution drifters have aided the measurement of some small scale fluctuation of velocity in a tidal shallow water estuary. Drifters are not perfect tracer because of they do not follow vertical motion, acts as filter which reducing the intensity of the true flow, inability to perfectly lock to water due to slip and effect of crossing trajectories. In order to verify that the drifters motion within the period of observation were driven by the underlying turbulence; the Lagrangian velocity spectra were examined. The power spectral densities of the velocities between 0.0001 and 0.5 Hz were well fitted with slope of 5/3 predicted by Kolmogorov's similarity hypothesis within the inertial subrange and were

similar to the Eulerian power spectrum previously observed within the channel. The observed velocities were unsteady and non-stationary.

The low frequency velocity fluctuations significantly influenced the decorrelation of the autocorrelation functions while the basic assumption for the Taylor's diffusivity estimate includes stationarity at the scale under consideration. Therefore, the use of a running mean with a time averaging window is recommended for removing the large scale fluctuations which are of interest. The method of segmentation produced consistent Lagrangian auto-correlation functions for short realisations with a time length at least twice the time of evolution of lowest frequency in the residual velocity.

The diffusivity scale of $K_{ss} = 0.0025 \pm 0.0012$ m^2/s and $K_{nn} = 0.0012 \pm 0.0005$ m^2/s were obtained from the stationary turbulent residual velocity. Dimensionless diffusivity values in the present study varied between 0.02 and 0.11 which is within the range of 0.005–7 obtained from the dye experimental data and smaller than the drifter spreading data values of ~ 0.13 and ~ 0.22 in and outside the tidal channel, respectively. Peak diffusivity was observed at the early part of the flood which corresponds to the peak horizontal mean velocity. The small scale diffusivity showed strong dependence ($R^2 > 0.9$) on the horizontal velocity and the fluctuation of eddy speed. The result here also show enhanced diffusivity caused by shear dispersion resulting from the interaction of large scale flow with the boundary geometries. The diffusivities scale locally by 4/3 power law following Okubo's scaling and the integral length scales as the 3/2 power law of the integral time scale.

The results of scaling herein suggest that the modelling of small scale mixing within tidal shallow estuaries can be approached from classical scaling analysis upon identifying pertinent parameters. However, this requires more experimental data set because of the orders of magnitude disparity between the existing mixing parameters (e.g. diffusivity) from large water bodies and the small tidal shallow water such as Eprapah Creek. The results show the applicability of high resolution Lagrangian drifter study to understanding transport and mixing in shallow estuarine water at small time and space scales. While the diffusivity estimates here do not separately quantify the diffusion by the 'true' turbulence and shear dispersion, ongoing analysis have been channelled to resolve individual contribution through cluster deployments.

References

1. Elder J (1959) The dispersion of marked fluid in turbulent shear flow. J Fluid Mech 5(04):544–560. doi:10.1017/S0022112059000374
2. Okubo A (1971) Oceanic diffusion diagrams. Deep Sea Res Oceanogr Abstr 18(8):789–802. doi:10.1016/0011-7471(71)90046-5
3. MacCready P, Geyer WR (2010) Advances in estuarine physics. Ann Rev Mar Sci 2:35–58. doi:10.1146/annurev-marine-120308-08101
4. Fischer HB, List EJ, Koh RC, Imberger J, Brooks NH (1979) Mixing in inland and coastal waters. Academic Press, London

5. Riddle A, Lewis R (2000) Dispersion experiments in UK coastal waters. Estuar Coast Shelf Sci 51(2):243–254. doi:10.1006/ecss.2000.0661

6. Poje AC, Özgökmen TM, Lipphardt BL, Haus BK, Ryan EH, Haza AC, Jacobs GA, Reniers A, Olascoaga MJ, Novelli G (2014) Submesoscale dispersion in the vicinity of the Deepwater Horizon spill. Proc Natl Acad Sci 111(35):12693–12698. doi:10.1073/pnas.1402452111

7. Schroeder K, Chiggiato J, Haza AC, Griffa A, Özgökmen TM, Zanasca P, Molcard A, Borghini M, Poulain PM, Gerin R, Zambianchi E, Falco P, Trees C (2012) Targeted Lagrangian sampling of submesoscale dispersion at a coastal frontal zone. Geophys Res Lett 39(11):L11608. doi:10.1029/2012GL051879

8. Torsvik T, Kalda J (2014) Analysis of surface current properties in the Gulf of Finland using data from surface drifters. In: Baltic international symposium (BALTIC), 2014 IEEE/OES, 2014, pp 1–9

9. Stocker R, Imberger J (2003) Horizontal transport and dispersion in the surface layer of a medium-sized lake. Limnol Oceanogr 48(3):971–982. doi:10.4319/lo.2003.48.3.0971

10. Tseng RS (2002) On the dispersion and diffusion near estuaries and around islands. Estuar Coast Shelf Sci 54(1):89–100. doi:10.1006/ecss.2001.0830

11. Spydell MS, Feddersen F, Olabarrieta M, Chen J, Guza RT, Raubenheimer B, Elgar S (2015) Observed and modeled drifters at a tidal inlet. J Geophys Res Oceans 120(7):4825–4844. doi:10.1002/2014JC010541

12. Suara K, Wang C, Feng Y, Brown RJ, Chanson H, Borgas M (2015) High resolution GNSS-tracked drifter for studying surface dispersion in shallow water. J Atmos Ocean Technol 32(3):579–590. doi:10.1175/JTECH-D-14-00127.1

13. Pinton J-F, Sawford BL (2012) A Lagrangian view of turbulent dispersion and mixing. In: Davidson P et al (eds) Ten chapters in turbulence. Cambridge University Press, Cambridge, pp 133–175

14. Volk R, Calzavarini E, Leveque E, Pinton J-F (2011) Dynamics of inertial particles in a turbulent von Kármán flow. J Fluid Mech 668:223–235. doi:10.1017/S0022112010005690

15. LaCasce J (2008) Lagrangian statistics from oceanic and atmospheric observations. In: Transport and mixing in geophysical flows. Springer, Berlin, pp 165–218. doi:10.1007/978-3-540-75215-8_8

16. LaCasce J, Bower A (2000) Relative dispersion in the subsurface North Atlantic. J Mar Res 58(6):863–894. doi:10.1357/002224000763485737

17. Taylor GI (1921) Diffusion by continuous movements. Proc Lond Math Soc 20:196–211

18. Suara K, Brown R, Wang C, Borgas M, Feng Y (2015) Estimate of Lagrangian integral scales in shallow tidal water using high resolution GPS-tracked drifters. In: E-proceeding of the 36th IAHR World Congress, The World Forum, Delft-The Hague

19. Chanson H (2008) Field observations in a small subtropical estuary during and after a rainstorm event. Estuar Coast Shelf Sci 80(1):114–120. doi:10.1016/j.ecss.2008.07.013

20. Trevethan M, Chanson H, Brown R (2008) Turbulent measurements in a small subtropical estuary with semidiurnal tides. J Hydraul Eng 134(11):1665–1670. doi:10.1061/(ASCE)0733-9429(2008)134%3A11(1665)

21. Chanson H, Trevethan M (2010) Turbulence, turbulent mixing and diffusion in shallow-water estuaries. Atmospheric turbulence, meteorological modeling and aerodynamics. Nova Science Publishers, New York, pp 167–204

22. Situ R, Brown RJ (2013) Mixing and dispersion of pollutants emitted from an outboard motor. Mar Pollut Bull 69(1–2):19. doi:10.1016/j.marpolbul.2012.12.015

23. Takasu T, Yasuda A (2009) Development of the low-cost RTK-GPS receiver with an open source program package RTKLIB. In: International symposium on GPS/GNSS, International Convention Center Jeju, Korea

24. Suara K, Brown RJ, Chanson H (2015) Turbulence and mixing in the environment: multi-device study in a sub-tropical estuary. Hydraulic model report CH series CH99/15, School of Civil Engineering, The University of Queensland

25. Goring DG, Nikora VI (2002) Despiking acoustic Doppler velocimeter data. J Hydraul Eng 128(1):117–126. doi:10.1061/(ASCE)0733-9429(2002)128:1(117)

26. Spydell M, Feddersen F, Guza R, Schmidt W (2007) Observing surf-zone dispersion with drifters. J Phys Oceanogr 37(12):2920–2939. doi:10.1175/2007JPO3580.1

27. Schafer RW (2011) What is a Savitzky–Golay filter? Sig Process Mag IEEE 28(4):111–117

28. Legleiter CJ, Kyriakidis PC (2006) Forward and inverse transformations between Cartesian and channel-fitted coordinate systems for meandering rivers. Math Geol 38(8):927–958. doi:10.1007/s11004-006-9056-6

29. Suara K, Brown R, Chanson H Turbulence measurements in a shallow tidal estuary: analysis based on triple decomposition. In: 19AFMC: 19th Australasian Fluid Mechanics Conference, 2014. Vol Paper 359. Australasian Fluid Mechanics Society, pp 1–4

30. Haza AC, Özgökmen TM, Griffa A, Poje AC, Lelong M-P (2014) How does drifter position uncertainty affect ocean dispersion estimates? J Atmos Ocean Technol 31(12):2809–2828. doi:10.1175/JTECH-D-14-00107.1

31. Xia H, Francois N, Punzmann H, Shats M (2013) Lagrangian scale of particle dispersion in turbulence. Nat Commun. doi:10.1038/ncomms3013

32. Ohlmann JC, LaCasce JH, Washburn L, Mariano AJ, Emery B (2012) Relative dispersion observations and trajectory modeling in the Santa Barbara Channel. J Geophys Res Oceans (1978–2012). doi:10.1029/2011JC007810

33. Qian Y-K, Peng S, Liang C-X, Lumpkin R (2014) On the estimation of Lagrangian diffusivity: influence of nonstationary mean flow. J Phys Oceanogr 44(10):2796–2811

34. Colin de Verdiere A (1983) Lagrangian eddy statistics from surface drifters in the eastern North Atlantic. J Mar Res 41(3):375–398. doi:10.1357/002224083788519713

35. Davidson PA (2004) Turbulence: an introduction for scientists and engineers. Oxford University Press, Oxford

36. Chanson H, Gibbes B, Brown RJ (2014) Turbulent mixing and sediment processes in peri-urban Estuariesin South-East Queensland (Australia). In: Wolanski E (ed) Estuaries of Australia in 2050 and Beyond. Springer, Berlin

37. Trevethan M, Chanson H (2009) Turbulent mixing in a small estuary: detailed measurements. Estuar Coast Shelf Sci 81(2):191–200. doi:10.1016/j.ecss.2008.10.020

38. Richardson LF (1926) Atmospheric diffusion shown on a distance-neighbour graph. In: Proceedings of the Royal Society of London Series A, containing papers of a mathematical and physical character, vol 110(756), pp 709–737